Spherical Nanoindentation Analysis with Irradiation Effects and Calibration with Machine Learning

Hwan-Jae Joo[a], Dong-Hyeon Kwak[a], and Yoon-Suk Chang[a*]
[a]*Department of Nuclear Engineering, Kyung Hee University, 1732 Deogyeong-daero, Giheung-gu, Yongin-si, Gyeonggi-do 17104, Republic of Korea*
[*]*Corresponding author: yschang@khu.ac.kr*

1. Introduction

Austenitic Stainless Steels (ASSs) which have high strength and ductility are the main material of Reactor Vessel Internals (RVIs). RVIs are degraded by the extreme environment and neutron irradiation. From microstructure defects, mechanical properties are changed. Irradiated material property was studied by Mecking-Kocks (M-K) with parametric equations [1].

Experimental studies have several limitations for investigating mechanical properties due to producing of irradiated specimen and irradiation pollution. Therefore, the nanoindentation test has been used to alternative procedure for evaluate mechanical properties.

A Finite Element Analysis (FEA) was conducted to observe irradiated material behavior from microstructure characters for As-Received (AR) and irradiated 304 ASSs [2]. To match with the experiment, irradiation material model parameters must be calibrated. Using machine learning reduces time, effort, and error [3].

In this study, material properties under AR and irradiated condition were simulated with the M-K theory and FEA. Parameters were calibrated by using machine learning comparing FEA and the experiment data. From the calibration result, the irradiation dose of each depth was analyzed to confirm the mechanical property effect from a depth dependency of irradiation level.

2. Microstructure Analysis

2.1 Review of material constitutive model

The dislocation-based flow stress (σ_f) is calculated from the shear stress (τ_f) with Taylor factor as following in Eq. (1). The relation of the flow stress on dislocation density is derived from the following Eqs. (2) and (3).

$$\sigma_f = M\tau \quad (1)$$

$$\sigma_f = \sigma_0 + \alpha\mu M b\sqrt{\rho_0 + \rho_{DL}} \quad (2)$$

$$\tau_0 = \alpha\mu b\sqrt{\rho_0} \qquad \tau_{DL} = \alpha_{DL}\mu b\sqrt{\rho_{DL}} \quad (3)$$

Where, b is the magnitude of the Burgers vector, ρ is the dislocation density, α is the strengthening factor of an obstacle, μ is the shear modulus, and σ_0, τ_0 are the stress of initial dislocation network.

Since Dislocation Loop (DL) was considered as the major irradiation defects, the quadratic sum was applied to represent in Eq. (4) [4].

$$\tau_{total} = \sqrt{(\tau_0)^2 + (\tau_{DL})^2} \quad (4)$$

From M-K theory, the evolution of dislocation density comes from production and annihilation of dislocations [5]. The production is related to the mean free path (λ). The annihilation is from the dynamic recovery (f). The microstructure-based plasticity behavior was used by a user subroutine UHARD as Eqs. (1) - (5).

$$\left(\frac{d\rho}{d\gamma}\right) = \left(\frac{d\rho}{d\gamma}\right)^{+} + \left(\frac{d\rho}{d\gamma}\right)^{-}$$
$$\left(\frac{d\rho}{d\gamma}\right)^{+} = \frac{1}{\lambda b}, \left(\frac{d\rho}{d\gamma}\right)^{-} = -f\rho \qquad \frac{1}{\lambda} = \frac{1}{d} + k\sqrt{\rho} \quad (5)$$
$$\left(\frac{d\rho}{d\gamma}\right) = \frac{d\rho}{M \cdot d\varepsilon} = \frac{1}{b \cdot d} + \frac{k}{b}\sqrt{\rho} - f\rho$$

where, d is grain size, k is product constant, f is annihilation constant, γ is shear strain.

2.2 Nanoindentation model

A numerical model of spherical nanoindentation simulation was created using the FEA package (ABAQUS) details in Figure. 1. A region between the indenter and specimen was refined mesh and was applied to 0.2 of friction coefficient.

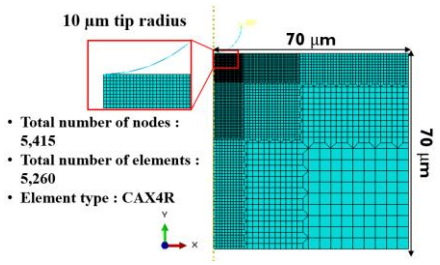

Fig. 1. FE model

3. Calibration Supported by Machine Learning

3.1 Data collection and preprocessing

Three parameters (a, f, k) were considered in each dose. Total of 144 analyses were performed for resulting Strain Energy (SE) and the maximum load (P_{max}) of load-depth curve. Among them, 48 data were randomly sampled as input dataset (a, f, k) and target data (SE, P_{max}) for training. The most optimum dataset was selected.

3.2 Ridge regression

Ridge Regression (RR) is an algorithm for regulating over or under-fitting of model and minimizing difference between each result of FEA and RR prediction. Using

this algorithm, optimized parameters were drawn out for calibration in AR and irradiated condition.

Two performances, Mean Absolute Percentage Error (MAPE) and R-squared (R^2), were used to evaluate the accuracy of ridge regressions in Table I. Where $\hat{y}_i$ is the prediction value, y_i is the true value, n is the number of samples, and $\bar{y}_i$ is the average of y_i.

$$MAPE = \frac{100\%}{n}\sum_{i=1}^{n}\left|\frac{\hat{y}_i - y_i}{y_i}\right| \quad (6)$$

$$R^2 = 1 - \frac{\sum_{i=1}^{n}(y_i - \hat{y}_i)^2}{\sum_{i=1}^{n}(y_i - \bar{y}_i)} \quad (7)$$

Table I: Performance evaluation

Variables	Performance	AR	10 dpa
Strain Energy	MAPE (%)	0.93	1.89
	R^2	0.96	0.94
Maximum Load	MAPE (%)	1.83	1.98
	R^2	0.93	0.98

4. Assessment of Analysis Results

4.1 Calibration results in AR and irradiated conditions

The calibration result is compared with experiment with AR and 10 dpa in Figure. 2 [6] and Table II. FEA results from the maximum load were 18.5% and 18.9% higher than experiment.

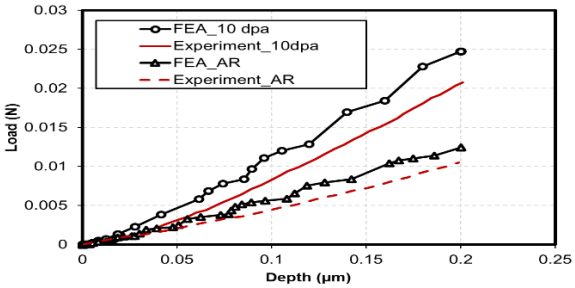

Fig. 2. Load-Depth Curve of each condition

Table II: Calibrated Parameters [1, 2, 4]

Variables	Values	Variables	Values
E (GPa)	200	d (mm)	48×10^{-3}
Poisson's ratio (υ)	0.3	α	0.1
σ_0 (MPa)	250	k	3.16×10^{-2}
ρ_0(mm^{-2})	1.0×10^{6}	f	3.16×10^{-2}
M	3.06	α_{DL}	0.2
μ (MPa)	77,000	k_{DL}	3.16×10^{-2}
b (mm)	2.54×10^{-7}	f_{DL}	3.16×10^{-2}

4.2 Depth dependency in nanoindentation analysis

The irradiation effect decreases as proton penetrates a test specimen. FEA which has different dose at several depth and 5 μm indentation was performed in Figure. 3. The result of depth dependency is less than 10 dpa and more than AR.

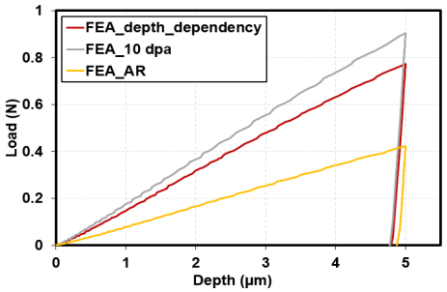

Fig. 3. Load-Depth Curve of depth dependency

5. Conclusions

In this study, microscale analyses and calibration with machine learning were conducted to investigate irradiation effects with depth dependences on ASSs.

(1) The differences in the predicted target dataset from RR and analysis results were derived as low as 2% under AR and irradiation condition. The R^2 value of more than 0.9 indicates higher prediction accuracy.
(2) Compared FEA and experiment at AR and irradiation effects, there were differences of 18.5% and 18.9% from the maximum load, respectively. From these results, it is necessary to study convergence of machine learning.
(3) The depth effect of irradiation was predicted from the FEA with each dose. The depth dependency of irradiation was observed from comparing of result.

ACKNOWLEGMENTS

This research was supported by Korea Institute of Energy Technology Evaluation and Planning (KETEP) grant funded by the Korea government (MOTIE) (No. 20191510301140).

REFERENCES

[1] Pokor, C, et al., Irradiation damage in 304 and 316 stainless steels: experimental investigation and modeling. Part I: Evolution of the microstructure, Journal of Nuclear Materials, Vol. 326 pp. 19-29, 2004.
[2] Kwak, D. H., Sim, J. M., and Chang, Y. S., Determination of Irradiated Stainless-Steel Properties and Its Effects on Reactor Vessel Internals, Proceedings of ASME 2020 Pressure Vessels & Piping Conference, August 3, 2020.
[3] Johannes Reiner, Reza Vaziri, Navid Zobeiry, Machine learning assisted characterisation and simulation of compressive damage in composite laminates, Composite Structures, Vol. 273, pp. 114-290, 2021.
[4] Monnet, G., Multiscale modeling of irradiation hardening: Application to important nuclear materials, Journal of Nuclear Materials, Vol. 508, pp. 609-627, 2018
[5] Bouquerel, J., Verbeken, K. and De Cooman, B. C., Microstructure-based model for the static mechanical behavior of multiphase steels, Acta Materialia, Vol. 54, pp. 1443-1456, 2006.
[6] J. S. Weaver, et al., Spherical nanoindentation of proton irradiated 304 stainless steel: A comparison of small scale mechanical test techniques for measuring irradiation hardening, Journal of Nuclear Materials, Vol. 493, pp. 368-379, 2017